Characterization and Correction of a Drift in Calibration of the TOPEX Microwave Radiometer

Christopher S. Ruf

***Abstract*—Characterization of the drift in the 18-GHz brightness temperature (TB) measured by the TOPEX microwave radiometer (TMR) is presented. The appropriate correction is not a constant drift but varies with TB. Using this correction results in a more accurate path delay retrieval that varies appropriately with cloud cover and surface wind speed.**

***Index Terms*—Microwave radiometry, ocean altimetry, satellite calibration.**

I. Introduction

The TOPEX microwave radiometer (TMR) is a nadir pointing spaceborne microwave radiometer that flies alongside the TOPEX altimeter to estimate variations in the integrated refractivity of the atmosphere due to water vapor and cloud liquid [1]. TOPEX was launched in August 1992. The TMR operates at 18, 21, and 37 GHz. Early post-launch calibration/validation of TMR performance demonstrated absolute calibration of its brightness temperature (TB) at all three frequencies of $\pm$1.5 K [5]. Subsequent studies using tide gauge comparisons detected a $\sim$2 mm/y mean global drift in TOPEX-derived sea level [4]. That drift was correlated with latitude in a manner that suggested a possible drift in the TMR wet path delay (PD) estimates. This was later corroborated by a series of intercomparisons between TMR and

1) ERS-1 and ERS-2 [8];
2) ground-based GPS [2];
3) SSM/I and radiosondes [3].

The intercomparisons all pointed to a drift of approximately 1.2 mm/y in the PDs produced by TMR between launch and late 1996.

The cause of the drift was isolated to the 18-GHz channel of TMR using a vicarious cold reference technique developed by [7]. In this earlier study, several principle characteristics of the 18-GHz drift were identified. They are summarized as follows.

1) The coldest TBs observed at 18 GHz rise from 123.5 K to 124.6 K between launch in August 1992 and December 1996, or 0.27 K/y. After December 1996, the drift stops and the coldest TBs remain steady at 124.6 K. Coldest TBs are believed to be a stable statistical property of globally distributed measurements and drifts are attributed to instrumental effects.
2) Immediately after launch, the difference between the mean cold space TBs while TOPEX is over coldest ocean ($\mathrm{TB} < 130$ K at 18 GHz) and over warmest land ($\mathrm{TB} > 280$ K at 18 GHz) is 0.5 K. The effect of Earth TBs on the measurement of cold space TB results from a small signal leakage through the calibration switch that switches between Earth and cold space viewing antennas. The 0.5 K difference corresponds to an isolation level in the calibration switch of approximately 25 dB.
3) The cold space difference decreases monotonically from 0.5 K to 0.25 K between launch and December 1996. A cold space difference of 0.25 K corresponds to an isolation level in the calibration switch of approximately 28 dB. After December 1996, the cold space difference remains steady at 0.25 K.

These characteristics of the 18-GHz drift will be used in the work presented here to develop a consistent model for the instrument drift. Based on this model, a correction algorithm is developed which can be applied to the 18-GHz TBs.

II. Instrument Drift Model

The TMR calibration switch consists of two latching ferrite circulators that combine to direct the input to the receivers from one of either the Earth viewing reflector antenna, the cold space viewing horn antenna, or a warm load waveguide matched termination. The effective brightness of the signals including leakage effects can be written as

$$T'_A = T_A(1 - L_{\mathrm{AW}}) + L_{\mathrm{AW}} T_W \tag{1a}$$

$$T'_C = T_C(1 - L_{\mathrm{CA}} - L_{\mathrm{CW}}) + L_{\mathrm{CA}} T_A + L_{\mathrm{CW}} T_W \tag{1b}$$

$$T'_W = T_W(1 - L_{\mathrm{WA}} - L_{\mathrm{WC}}) + L_{\mathrm{WA}} T_A + L_{\mathrm{WC}} T_C \tag{1c}$$

where
- T_A Earth viewing antenna temperature;
- T_C cold space brightness;
- T_W warm load temperature;
- L_{jk} level of leakage from source k into measurement j.

The raw digital counts are given by

$$C_i = G\left(T_W - T'_i\right) \tag{2}$$

where $i = A$ (antenna), C (cold sky), or W (warm load), and G is the instrument gain in units of Counts/Kelvin. Combining (1) and (2) and solving for T_A gives

$$T_A = T_W - \frac{C_A}{(1 - L_{\mathrm{AW}})(C_C - C_W)}\left(T'_W - T'_C\right). \tag{3}$$

Several assumptions can be made about the relationship between leakage terms. The two terms L_{CA} and L_{WA} are likely equal since they both arise from leakage of the signal from the main reflector antenna when the upper circulator is switched to the calibration sources. The two terms L_{CW} and L_{WC} which account for isolation between the cold sky and warm load arms of the lower circulator, will be assumed to be equal and stable over time since there is no direct evidence otherwise. In (1a), a third source term with leakage L_{AC} is not included because it would be $\sim$2 orders of magnitude below the other leakage terms considered here due to two cascaded blocking circulators.

Based on the three characteristics of the drift noted in Section I, the conjecture is that the drift in coldest 18-GHz TB occurred because of an unaccounted for decrease in the leakage term L_{CA}. Any changes in L_{CA} would likely be associated with changes in L_{AW} since they correspond to the isolation of the same circulator when it is in its alternate latched states. Direct estimates of L_{AW} using flight data, or detection of drifts in L_{AW} over time, are much more difficult and have been unsuccessful because the source of the leakage signal T_W is much less variable than the source of leakage T_A with which L_{CA} is associated. It is hypothesized that a decrease in L_{CA} by ΔL dB would be accompanied by a corresponding increase in L_{AW} by ΔL dB. The reasoning behind this is as follows: A latching circulator is driven into its "latched" operating states by driving the magnetic core material into opposite extremes of its hysteresis curve. The observed decrease in L_{CA} over the first four years of the mission is consistent with greater saturation of the core, i.e., settling further along the hysteresis curve when the circulator is latched in the position to observe the warm load and cold space calibration sources. This may have been caused by a change in the driver

Manuscript received April 25, 2001; revised July 25, 2001. This paper presents the results of one phase of research conducted in part with support from the Jet Propulsion Laboratory (JPL), California Institute of Technology. JPL is under contract with the National Aeronautics and Space Administration.

The author is with the Department of Atmospheric, Oceanic, and Space Sciences, University of Michigan, Ann Arbor, MI 48109 USA (e-mail: cruf@umich.edu).

Publisher Item Identifier S 0196-2892(02)02123-X.

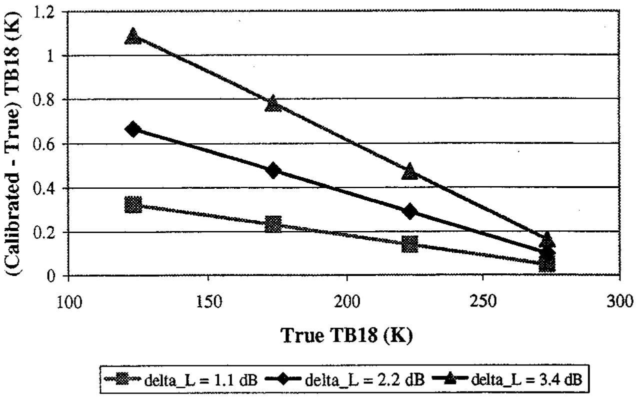

Fig. 1. Error in calibrated TBs due to an unaccounted for change in the isolation of the latching ferrite circulator that switches between the Earth viewing main reflector antenna and either of the warm load or cold space horn.

circuit that excites the external magnetic field around the core. If penetration into one end of the hysteresis curve has increased, and if a corresponding change in the driver circuit in the reverse direction has not occurred, then it is reasonable to assume that there will be a decrease in penetration along the hysteresis curve in the alternate latched state. The validity of the assumption that the changes are equal in magnitude is considered below.

The sensor data record (SDR) ground processing software for TMR calibration implicitly assumes that all circulator leakages are constant at -24.5 dB throughout the mission. The effect of this assumption on calibration error can be evaluated. Simulated digital counts are generated using (1) and (2) with changing values for $L_{\rm CA}$ and $L_{\rm AW}$ and assuming typical values of $T_W = 300$ K and $T_C = 40$ K. T_A is then estimated from the data using (3) but assuming constant values of -24.5 dB for all leakages. The results are shown in Fig. 1 for $\Delta L = 1.1, 2.2,$ and 3.4 dB. At $T_A = 123.5$ K (the true cold reference), calibration error is seen to increase to 1.1 K as ΔL increases to 3.4 dB. In addition, the difference between measured cold space brightness, given by (1b), while over a cold or warm Earth decreases from $\sim$0.5 K to 0.25 K as ΔL increases from 0 to 3.4 dB. Both of these characteristics are consistent with the drift indicators described above. Note that the error in calibration decreases linearly with T_A and approaches zero as T_A approaches T_W. This behavior is consistent with results reported by Eymard (*personal communication*, 2000) in which long term averages of high TMR TBs at 18 GHz over the Sahara desert do not exhibit the calibration drift.

The validity and significance of the assumption that $L_{\rm AW}$ decreases by ΔL as $L_{\rm CA}$ increases by the same amount can be tested. If $L_{\rm AW}$ is assumed to decrease only half as much as $L_{\rm CA}$ increases, then a 3.4-dB increase in $L_{\rm CA}$ will result in a calibration error of 0.64 K at $T_A = 123.5$ K (versus a 1.1 K error if they change equally). In order to reproduce the 1.1 K observed drift in cold T_A calibration in this case, $L_{\rm CA}$ needs to increase by 6.0 dB. The variation in calibration error versus T_A will then also behave similarly to the 3.4 dB curve in Fig. 1. However, a 6.0 dB increase in $L_{\rm CA}$ will also result in a change in the difference between measured cold space brightness over cold and warm Earth from 0.5 K to 0.13 K. This is a larger change than was actually observed. On the other hand, if $L_{\rm AW}$ is assumed to decrease twice as much as $L_{\rm CA}$ increases, then a 1.9 dB increase in $L_{\rm CA}$ will produce a shift in T_A calibration that is similar to that observed. But the difference between measured cold space brightness over cold and warm Earth will change from 0.5 K to 0.34 K, which is a smaller change than was observed. Thus, the assumption that $L_{\rm CA}$ and $L_{\rm AW}$ change with similar magnitudes in opposite directions is more consistent with the observations. It is difficult to precisely estimate the difference in cold space brightness over cold and warm Earth so an exact relationship between changes in $L_{\rm CA}$ and $L_{\rm AW}$ can't be determined. However, the relationship between the two changes have very little effect on the overall prediction of shifts in T_A calibration versus T_A, provided the change in $L_{\rm CA}$ is adjusted to produce a 1.1 K shift in T_A at 123.5 K. Therefore, the overall effect on the T_A calibration correction is not significant.

The instrumental drift mechanism that will be assumed is then the following.

1) $L_{\rm CA}$ decreases from -24.5 dB to -27.9 dB between launch and December 1996 and then remains steady at -27.9 dB after that.
2) $L_{\rm AW}$ increases from -24.5 dB to -21.1 dB over the same time and then remains steady at -21.1 dB.
3) $L_{\rm CW}$ and $L_{\rm WC}$ are both constant at -24.5 dB throughout the mission.

III. Algorithm for Correcting TMR 18-GHz TBs

The change in T_A calibration depends nearly linearly on the dB value of the leakage. For this reason, it is assumed that $L_{\rm CA}$ increases linearly over time from 24.5 dB at launch to 27.9 dB at the end of December 1996. The effect of an incremental change in $L_{\rm CA}$ by $\sim$1.1 dB per step is shown in Fig. 1. The slope and y-intercept of the T_A calibration error shown in the figure were determined for each value of ΔL. A fourth default condition is assumed that slope $=$ y-intercept $= 0$ at $\Delta L = 0$. Linear regressions were performed relating the slope and y-intercept of the calibration error to ΔL, giving

$$\Delta T_A = c_0 + c_1 T_A \tag{4a}$$
$$c_0 = 0.5431\Delta L - 0.027\,60 \tag{4b}$$
$$c_1 = -0.001\,825\Delta L + 0.000\,010\,63 \tag{4c}$$

where ΔL is in decibels. Note that ΔT_A is the positive calibration error in the TMR geophysical data records (GDRs) at 18 GHz and so should be subtracted from the GDR value. In other words, the appropriate correction algorithm is given by

$$TB18_{\rm corrected} = TB18_{\rm GDR} - \Delta T_A. \tag{5}$$

In practice, the GDR value for TB18 can be used in place of T_A in (4a). The time history of ΔL is a linear ramp during the period of drift, followed by a constant, or

$$\Delta L(t) = 0.819\,26^{*} t \text{ for } 0 \le t < 4.15 \text{ years} \tag{6a}$$
$$\Delta L(t) = 0.819\,26^{*} 4.15 \text{ for } 4.15 \text{ years} \le t \tag{6b}$$

where t is the elapsed time since launch (in August 1992) in units of years.

IV. Discussion and Conclusions

The effect of the 18-GHz channel cold reference TB drift on the retrieved PD is illustrated by considering a sample of measurements by TMR. The TB samples at nearest approach to Lampedusa Island (LAT 35.4N, LON 13.1E) were selected from each 10-day cycle of the TOPEX orbit during the first four years of the mission. This provides a range of PDs between 3 and 25 cm and includes both clear and cloudy conditions and low to moderate wind speeds. For illustrative purposes here, it is assumed that this distribution of TBs occurred during or after the fouth year of the mission and so includes the maximum possible drift in the 18-GHz channel. Beginning with these TBs, the PD was estimated in two ways. First, the TBs were input to the PD retrieval algorithm without correction for the 18 GHz drift and then the PDs were all corrected with a constant 5.0-mm bias correction ($= 4.15$ yr $\times$ 1.2 mm/y). Alternatively, the individual TBs at 18 GHz were first corrected for their drift, using (4)–(6), and then the corrected TBs were input

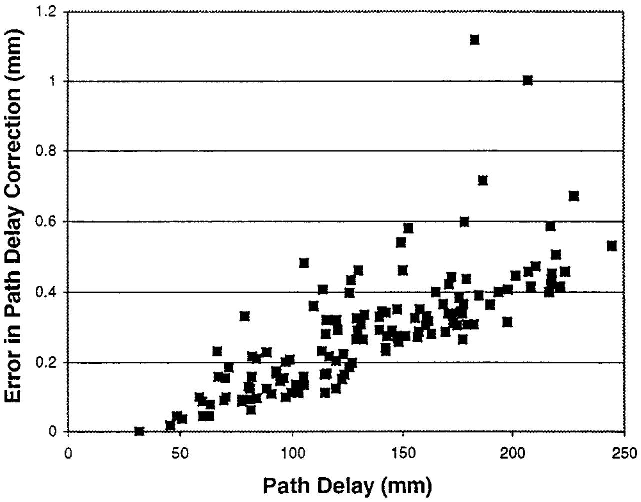

Fig. 2. Error in path delay (PD) retrieval if a simplified 1.2 mm/y correction is applied for all values of PD rather than correcting the TB at 18 GHz directly and then reprocessing the TBs through the PD retrieval algorithm. Data is selected from TMR overpasses near Lampedusa Island (LAT 35.39N, LON 13.10E) during 1992–1996.

to the PD retrieval algorithm. The difference between these two PD estimates is shown in Fig. 2 as a function of the latter (more accurate) PD.

In Fig. 2, a large majority of the differences cluster in a relationship that is roughly linear with PD. This cluster forms a distinct lower bound on the differences (ranging from no difference at very low PDs to a difference of approximately 0.5 mm at $\mathrm{PD} = 250$ mm). The samples in the cluster generally correspond to cloud free and low wind conditions. In these cases, there is nearly a linear relationship between the TBs at 18, 21, and 37 GHz and the PD [5]. Therefore, calibration biases in TB at 18 GHz will be linearly related to errors in PD. One simple improvement on a blanket 1.2 mm/y correction to the PDs might, then, be to incorporate this additional linear correction as a function of PD. However, such an improvement will not properly handle the numerous outlier points in Fig. 2 that lie above the lower bound cluster. These points arise from cloudy and/or higher wind conditions in which the relationship between TBs at each frequency cannot be explained by PD alone. Differences of 0.5–1.1 mm occur at PDs values well below the 250 mm maximum and in a manner not well correlated with PD. In these cases, it is best to reapply the full TMR PD retrieval algorithm to the drift corrected TBs.

A correction algorithm has been developed for the drift in calibration of the 18-GHz TMR channel. The resulting correction to TB varies linearly with TB and is greatest at lower TBs, dropping to zero when TB equals the physical temperature of the on board reference load. Given that the TB at 18 GHz that is typically measured by TMR on orbit over ocean only ranges over approximately 126–170 K, a constant drift correction of 0.27 K/y during the first four years of the mission is likely adequate for most purposes. A constant drift of this magnitude roughly corresponds to a constant drift in the retrieved PD of 1.2 m/y. However, use of a constant PD correction is found to result in small but systematic errors in the PD at the 1-mm level that are correlated with PD, with cloud cover, and with wind speed. Since all of these characteristics can have spatial scale sizes that are significantly greater than the individual TMR sample spacing of 45 km, the effects of these systematic errors can be important even though the magnitude of the errors is an order of magnitude smaller than the individual sample error. For this reason, it is recommended that, for highest quality PD retrievals, the drift correction be applied to 18-GHz TBs and then the corrected TBs be reprocessed through the PD retrieval algorithm.

References

[1] L. Fu, E. J. Christensen, C. A. Yamarone, Jr., M. Lefebvre, Y. Menard, M. Dorrer, and P. Esudier, "TOPEX/Poseidon mission overview," *J. Geophys. Res.*, vol. 24, pp. 24 369–24 382, 1994.

[2] B. J. Haines and Y. Bar-Sever, "Monitoring the TOPEX microwave radiometer with GPS: Stability of columnar water vapor measurements," *Geophys. Res. Lett.*, vol. 25, no. 19, pp. 3563–3566, 1998.

[3] S. J. Keihm, V. Zlotnicki, and C. S. Ruf, "TOPEX microwave radiometer performance evaluation, 1992–1998," *IEEE Trans. Geosci. Remote Sensing*, vol. 38, pp. 1379–1386, May 2000.

[4] G. T. Mitchum, "Monitoring the stability of satellite altimeters with tide gauges," *J. Atmos. Ocean. Technol.*, vol. 15, no. 3, pp. 721–730, 1998.

[5] C. S. Ruf, S. J. Keihm, B. Subramanya, and M. A. Janssen, "TOPEX/POSEIDON microwave radiometer performance and in-flight calibration," *J. Geophys. Res.*, vol. 99, no. C12, pp. 24 915–24 926, 1994.

[6] C. S. Ruf, S. J. Keihm, and M. A. Janssen, "TOPEX/POSEIDON microwave radiometer (TMR): I. Instrument description and antenna temperature calibration," *IEEE Trans. Geosci. Remote Sensing*, vol. 33, pp. 125–137, Jan. 1995.

[7] C. S. Ruf, "Detection of calibration drifts in spaceborne microwave radiometers using a vicarious cold reference," *IEEE Trans. Geosci. Remote Sensing*, vol. 38, pp. 44–52, Jan. 2000.

[8] J. Stum, "A comparison of the brightness temperatures and water vapor path delays measured by the TOPEX, ERS-1, and ERS-2 microwave radiometers," *J. Atmos. Ocean. Technol.*, vol. 15, no. 4, pp. 987–994, 1998.

The Line Segment Match Method for Extracting Road Network From High-Resolution Satellite Images

Wenzhong Shi and Changqing Zhu

***Abstract*—This paper presents an approach, with emphasis on the newly proposed line segment matching method, for extracting urban road networks from high-resolution satellite images. The approach is based on the characteristics of the images, knowledge about road networks, and the related mathematical models. The approach is applied to several images of urban areas and is proved to be effective in both visual effect and positional accuracy.**

***Index Terms*—High-resolution satellite image, line segment matching method, mathematical morphology, road network extraction.**

I. Introduction

Data extraction from remotely sensed images is the focus of research issues in, for example, automatic mapping and GIS data capture. Features extracted from images can be either linear features, such as roads,

Manuscript received November 8, 2000; revised September 4, 2001. This work was supported in part by the Research Grants Council of the Hong Kong SAR (Project PolyU 5071199E) and The Hong Kong Polytechnic University (Project 1.34.9709).

W. Shi is with the Department of Land Surveying and Geo-Informatics, The Hong Kong Polytechnic University, Kowloon, Hong Kong.

C. Zhu is with the Department of Land Surveying and Geo-Informatics, The Hong Kong Polytechnic University, Kowloon, Hong Kong and also with The Institute of Surveying and Mapping, Information Engineering University, Zhengzhou 450052, China.

Publisher Item Identifier S 0196-2892(02)02130-7.